Journal of Thermal Engineering
Yildiz Technical University Press, Istanbul, Turkey
Vol. 1, Special Issue 2, No. 7, pp. 636-646, February, 2015.

http://eds.yildiz.edu.tr/journal-of-thermal-engineering/Articles
Manuscript Received May 28, 2015; Accepted June 02, 2015

This paper was recommended for publication in revised form by Editor in Chief Ahmet Selim Dalkilic

NATURE INSPIRED OPTIMAL DESIGN OF HEAT CONVEYING NETWORKS FOR ADVANCED FIBER-REINFORCED COMPOSITES

Mahmoud Hamadiche
Claude Bernard Lyon I University
Lyon, France

***Natalya Kizilova**
ICM, Warsaw University
Warsaw, Poland

Keywords: Heat transfer, fiber reinforced composites, optimal design, nature inspired solutions, MEMS devices
** Corresponding author: Natalya Kizilova, Phone:+480518528485, Fax:+480624354221*
E-mail address: n.kizilova@gmail.com

ABSTRACT

A concept of composite materials reinforced by branching micro or nanotubes optimized for both heat transfer and strength of the material is presented. Numerous examples of reinforcement by branched fibers in cells, tissues and organs of plants and animals are studied. It is shown orientation of the fibers according to principals of the stress tensor at given external load is the main principle of optimal reinforcement in nature. The measurement data obtained on venations of the plant leaves revealed clear dependencies between the diameters, lengths and branching angles that correspond to delivery of the plant sap to live cells of the leaf with minimal energy expenses. The mathematical problem on geometry of asymmetrical loaded branched fibers experienced minimal maximal stress is solved. Heat propagation in the fibers is described by generalized Guyer-Krumhansl equation. It is shown the optimality for the heat propagation, fluid delivery and structural reinforcement are based on the same relations between the diameters, lengths and branching angles. The principle of optimal reinforcement is proposed for technical constructions, advanced composite materials and MEMS devices.

INTRODUCTION

Biological tissues are mostly presented by composite materials reinforced by fibers or tubes conveying biological fluids to and from the live cells (Fung, 1981). In animal tissues the arterial, venous, lymphatic vessels convey arterial or venous blood and lymph providing mass and heat distribution in the organs and within the organisms. The branched systems of airways supply flow of air inside and outside the lung providing the exchange of O_2 and CO_2 as well as heat exchange and thermoregulation. In plant tissues the xylem vessels provide xylem sap motion from roots to leaves, while phloem vessels conduct concentrated solution of polysaccharides synthesized in the leaves to the growing flowers, fruits, seeds and accumulating organs. The conducting systems of plants also serve for heat exchange and high-speed signaling based on the concentration waves propagated along the conducting vessels (Kizilova and Posdniak, 2005). In both animal and plant tissues the conducting systems are presented by branching pipelines (Fig.1).

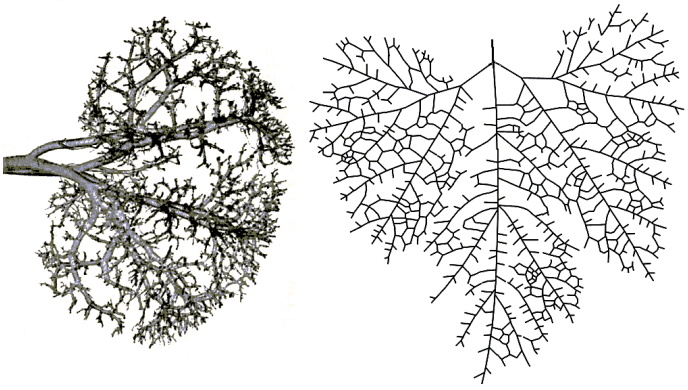

FIGURE 1 EXAMPLES OF ARTERIAL VASCULATURE (A) AND CONDUCTING SYSTEM OF PLANT LEAF (B)

As it was shown in numerous experimental studies and observations, geometry of the pipelines is determined by certain relationships between the diameters of the pipes in the bifurcations (Murray, 1926a; 1926b), and between the diameters and branching angles (Rosen, 1967; Weibel, 1963; La Barbera, 1990; Kizilova and Popova, 1999; McCulloh, Sperry and Adler, 2003)

$$d_0^3 = d_1^3 + d_2^3 \ , \tag{1}$$

$$\cos(\alpha_1) = \frac{(1+\xi^3)^{4/3} + 1 - \xi^4}{2(1+\xi^3)^{2/3}}, \qquad \cos(\alpha_2) = \frac{(1+\xi^3)^{4/3} + \xi^4 - 1}{2\xi^2(1+\xi^3)^{2/3}}. \tag{2}$$

It is amazing the principles of construction of fluid-conveying networks in animal and plant tissues and organs are the same, though the blood vessels and airways are soft and distensible, while the conducting elements in plants are rigid and possess porous walls and partitions (Kizilova, 2008). Theoretical substantiation of (1) is based on Murray's model of the optimal tube providing steady flow of a viscous fluid at total minimal energy expenses W so that

$$W = Q^2 Z \to \min, \quad \text{at} \ \ V = \pi R^2 L = \text{const}, \tag{3}$$

where Q=const, $Z = 8\eta L / (\pi R^4)$.

Solution of the optimization problem (3) gives the relation $Q \sim R^3$ for the optimal tube. It means for the bifurcation of three optimal tubes with diameters $d_{0,1,2}$ the relationship (1) follows from the mass conservation law. Since in the Poiseuille flow the wall shear stress (WSS) is

$$\tau_w = -\frac{4\mu Q}{\pi R^3},$$

in the optimal tube with $Q \sim R^3$ the WSS will be constant. It implies when the WSS is maintained at some constant level during the vessel growth and development, the optimal vessel will grow. It is approved the mechanosensory cells in the innermost endothelial layer of the blood vessels can estimate the WSS and transfer information on it into the inner layer composed of active smooth muscle cells (Zaragoza, Márquez and Saura, 2012). In that way, the blood vessel segments which are locally optimal to the steady flow can be developed. It is interesting; the relationship (1) is also a necessary condition of global optimality of the binary system of tubes (Chernousko, 1977; Kizilova, 2005a). Murray's law (1) has been generalized for the case of the steady viscous flow through the rigid tubes with permeable walls (Kizilova, 2005). It was shown, when $R / L \le 1$, the solution of the optimization problem (3) for the porous flow is also given by (1).

The relationship (2) also follows from the minimal energy loss principle (Rosen, 1967). As is was shown in numerous measurements, the correspondence between the theoretical and statistical data is very good in mean values, while some dispersion proper to biomedical data is presented. Detailed computations on the optimal branched angles and some configurations with deviation from the optimal ones revealed the increase in the energy loss in the most deviated stated does not exceed 10% (Kizilova, 2004b).

Transportation networks also serve for strength of the organ and organisms. The blood vessel vasculatures with different asymmetry of their branching support the shape and volume of soft inner organs (spleen, kidneys, liver, etc.) (Fig.2 a,b) as well as systems of veins keep the plant leaves unfolded and strong enough against wind, rain and other mechanical loads (Fig.2b).

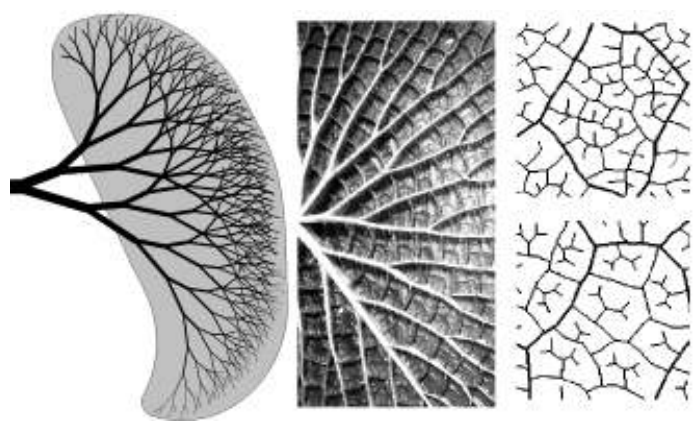

a b c

FIGURE 2 THE SHAPES AND SIZES OF INNER ORGANS SUPPLIED BY BRANCHED SYSTEM OF TUBES WITH $\xi = 0.8$ (A) AND VENATION OF THE **LARGER (B) AND THE SMALLER (C) LEAF VEINS**

In the solid tissues like bones and teeth the families of trabeculae orthogonal to the loaded surface (i.e. elongated according to the directions of maximal compression) and the orthogonal family of trabeculae located according to the directions of maximal extension in the tissue effectively work against extension and compression loads, while the non-working substance is dissolved and deleted producing the lightweight design (Fung, 1981). Main principle of biological growth is connected with elongation of cells and extracellular reinforcing structures (trabeculae in bones, sclerenchyma and collenchyma in plants and others) according to principals of the stress tensor at given external load. When the external load varies changing the stress field, the reinforcing system is remodeled keeping the optimal density and orientation for new

load conditions by active biological feedbacks. As a result, the uniform pattern of trabeculae in infant bones transform into clear body-specific orthogonal families of trabeculae, as well as tree trunks demonstrate straight or spiral grains depending on the permanent wind load (Leelavanichkul and Cherkaev, 2004). The corresponding theoretical model of bone as adaptive material has been developed (Cowin, 1989), but its practical implementation into the strategies of the in vivo growth control for tissue engineering purposes or into the smart materials with stress-dependent properties remains a challenge (Kizilova, 2012). It is important that the principles of biological growth discovered in animals and plants are the same in spite of the phylogenetic development of plants and animals had been separated since early stages of evolution when both types of live matter were presented by single animal and single plant cells and did not possess any macroscopic transportation and reinforcing structures.

Most biological tissues are composite materials formed by layers with different properties, viscoelastic solid porous structures and fibre reinforced materials with different structural patterns (Fung, 1981). The layered structures composed according to the external load can be found in cartilage. Coordinated growth of skeletal muscles and bones is provided by extension of the bones and muscles which are in parallel connection. The bones, cartilage, ligaments and other collagen structures possess piezoelectric properties, and electric fields generated in the loaded collagen fibers strongly influence growth direction and intensity (Fukada and Yasuda, 1957; Avdeev and Regirer, 1985).

In human skin the collagen fibers provide asymmetry in the skin distensibility depending on its natural loading. The collagen fibers in dermis and epidermis are oriented according to principals of stress tensor and provide maximal distensibility along the so-called Langer's lines and maximal rigidity along the orthogonal families (Langer, 1861). The same orientation of fibers has beet detected in the vascular cambium of trees (Kramer, 2002). Orientation of wood grains on the debarked surface of trunks and stems correspond to two families of fibers oriented according to the stress field. The outer layer of blood vessels (adventitia) is reinforced by two oppositely directed spiral families of collagen fibers (Holzapfel, Gasser and Ogden, 2006). The chords preventing the heart valves from outwards movement are also branched structures distributing the load uniformly along the leaflets of the valves. It is important the fibers in skin and other collagen tissues possess branching structure and are weaved in the textures of different density, anisotropy and strength (Fig.3).

The branching fibers have been found at the micro scale in tendon (Birk, et al., 1989), epithelium (Brownfield, Venugopalan and Lo, 2013), myocardial and many other tissues. In the myocardial tissues the branching are formed by myofibrils, not by collagen fibers. In that way, branching structures are proper to different types of cells and proteins. The branched nanostructures form cytoskeleton and serve for strength of animal cells and active intercellular transport by molecular motors (Kizilova, 2011). Probably, the branched fibers allow distribution information and cargo carried by the molecular motors more uniformly, just as along the side roads without jumping between the fibers.

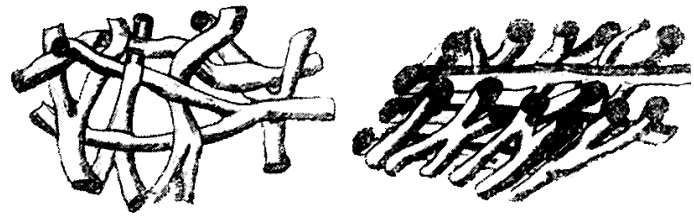

a b

FIGURE 3 THE PATTERNS OF BRANCHING COLLAGEN FIBERS IN HUMAN ARTERIAL WALL OF ELASTIC TYPE (A) AND IN THE SKIN (B)

In the tissues, organs and organisms of animals and plants the reinforced structured are loaded by pointed forces, pressures and shear forces. In the presence of the gravity field the efficiency of the branched rigid structures is an important constituent of the strength and durability of the general construction. According to the Schwendener's theory, the shape of plants is based on the concept of maximum strength (Schwendener, 1874; Schwendener, 1878). The mechanical structure of plants is determined by their ability for gravity recognition. Positive gravitropism of shoots and negative gravitropism of roots are determined by sedimentation of statoliths in the gravity field and polar transport of the plant hormone auxin. Distribution of the small branches in the crown is determined by maximizing its effective leaf area (Honda, 1978). Total leaf mass M_L is related to the diameter D of trunk as $M_L \sim D^2$ (Niklas and Spatz, 2004). Therefore, the relations between different organs in plants are determined by mechanical (stress-strain) and hydraulic (water supply) factors.

The principles of reinforcement are similar in the plant and animal tissues and based on minimal total energy expenses at a given body mass/volume and external load. The nature-inspired principles of reinforcement by micro and nanofibers in cells, tissues and organs can be used for elaboration of novel functional composite materials with optimal structural and transport properties, as well as in MEMS, fuel cells, micro heaters/coolers and other advanced technological units. Since bifurcating fibers, nano and microtubes are proper to live nature, their branching patterns deserve detailed consideration from the mechanical point of view.

Recently significant attention is paid for manufacture the branched micro and nanofibers for technical applications. The electrospun nanofibers with different density and length of the side branches has been elaborated (Yarin, et al., 2005; Gevorkyan, 2014). Chitosan fibers that have been found important as biodegradable scaffolds for tissue engineered skin

production can also be synthesized in the branched forms, which influence their degradation rate, adhesively for proteins and cells (Aggarwal and Matthew, 2009). The synthesized networks of branched nanofibes and morphology of the single branch are presented in Fig. 4a and Fig.4 b accordingly. Novel technologies allow obtaining the super strong multi-walled carbon nanotubes with single and several side branches (Fig.5.a).

Since the synthesized networks of branched nanotubes, fibers and ribbons can be used for reinforcement in the advanced composites, the high heat, electric charge and mass conductivity of such structures can be used. The resulted manufactured materials would possess unique high thermal conductivity or charge conductivity properties as well as high strength provided the reinforcing network has certain optimal design based on the laws of reinforcement in live nature.

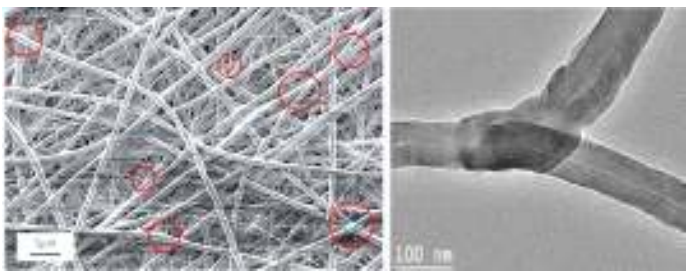

a b

FIGURE 4 IMAGES OF THE NETWORK OF BRANCHED NANOFIBERS (FROM GEVORKYAN, ET AL., 2014) (A) AND OF THE SINGLE Y-SHAPED JUNCTION OF NANOFIBERS (FROM BOSKOVIC, ET AL., 2004) (B)

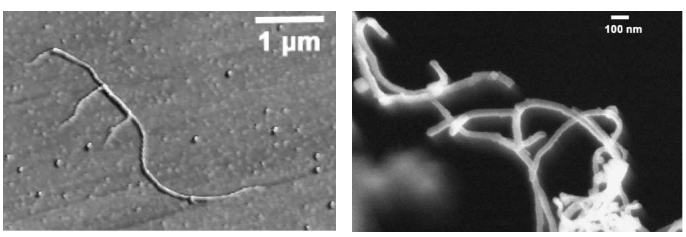

a b

FIGURE 5 ATOMIC FORCE MICROSCOPY IMAGE OF A Y-JUNCTION NANOTUBE WITH TWO SIDE BRANCHES (A) AND A NETWORK OF THE BRANCHED TUBES (B) (FROM HEYNING, 2005)

Summarizing the above presented data on fiber reinforcement in nature, one can conclude both plants and animals use the same main principles of mechanical construction of their tissues and organs, namely

- Reinforcement by relatively rigid fibers/tubes located according the principles of the stress tensor at given external mechanical load;
- The matrix material is viscoelastic/viscoplastic and serves for stress redistribution preventing crack generation or sticking crack propagation at fibers/tubes;
- The embedded tubes serve for reinforcement of the material as well as for mass and heat transport purposes;
- The branching fibers/tubes are commonly used at macro, micro and nano scales;
- Multi-criteria optimization of the network of reinforcing tubes for both mechanical strength and heat/mass conductivity must be done, which is the subject of the present work.

OPTIMAL DESIGN OF THE NETWORKS OF HEAT CONDUCTING FIBERS

The hear flux in the micro and nanofibers can be described by Guyer-Krumhansl equation in the form

$$\tau \frac{d\vec{q}}{dt} + \vec{q} = -\lambda \nabla T + \chi \nabla^2 \vec{q} \,. \tag{4}$$

At $\tau = 0,\ \chi = 0$ (4) transforms into the Fourier law for stationary heat flux.

Let introduce the characteristic values t^*, L, T^*, q^* for the time, space, temperature and heat flux values. Then (4) can be rewritten in the non-dimensional form

$$\frac{\tau}{t^*}\frac{d\vec{q}^\circ}{dt^\circ} + \vec{q}^\circ = -\frac{\lambda T^*}{L q^*}\nabla T^\circ + \frac{\chi}{L^2}\nabla^2 \vec{q}^\circ \,, \tag{5}$$

where the nondimensional valued are marked by circle upper script.

When $\tau << t^*$ the relaxational effects may be neglected. At the small space scales the last term in the left hand site (5) is negligible in comparison to the terms in the right hand side part of (5), so (5) reduces to the Poiseuille type equation (Alvarez, Jou and Sellitto, 2009)

$$\nabla T^\circ = \kappa \nabla^2 \vec{q}^\circ \tag{6}$$

where the nondimensional heat flux $\vec{q}^\circ$ is analogous to fluid velocity driven by the temperature gradient, which is analogous to the pressure drop for the fluid flow, $\kappa = \chi q^* / \lambda T^* L$ is the damping coefficient equivalent to the kinematic viscosity of the fluid.

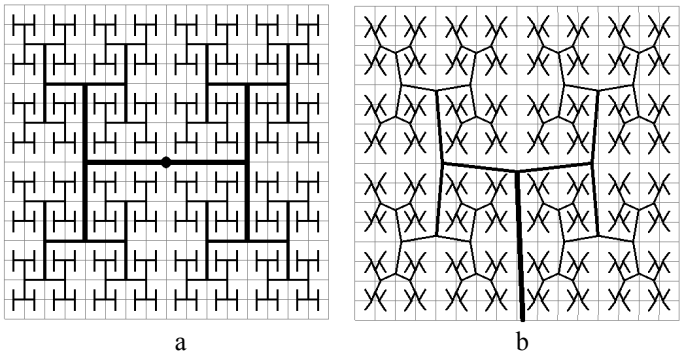

FIGURE 6 BRANCHING NETWORKS FOR SYMMETRICAL (A) AND MINIMAL TOTAL ENERGY EXPENSES (B) DESIGNS

In that way solution of the optimization problem (3) for the branching network of the heat conducting micro or nanowires and the relationships (1), (2) must be fulfilled. Like for the fluid flow case, the conditions of local optimality of the tube/wire will coincide with necessary conditions of global optimality of the network in the meaning of the minimal total energy expenses for the fluid/heat flux and structural support of the network (material and other expenses). It gives example of the functionally perfect nature inspired design with optimal branching angles α_1, α_2 (Fig.6 b) instead of geometrically perfect engineered design with $\alpha_{1,2} = 90^\circ$ (Fig.6a).

OPTIMAL DESIGN OF LOADED Y-SHAPED FIBERS

Let us consider three bars of circular cross sections composed a bifurcation OABC (Fig. 6). The lines OA, AB and AC belong to the same plane, the coordinates of the points are O(0,0), A(x,0), B(a,b_1), and C(a,-b_2), the diameters and lengths of the bars are d_0, d_1, d_2 and L_0, L_1, L_2 correspondingly. The bar OA is rigidly clamped at the cross section x=0, y=0, the bars are loaded by point forces $\vec{F}_{1,2}$ located perpendicularly to the plane 0xy and applied in the points B,C (Fig.7). Let us find out the branching design when at the given volume of the bifurcation

$$V = \frac{\pi}{4}\left(d_0^2 L_0 + d_1^2 L_1 + d_2^2 L_2\right), \tag{7}$$

where the maximal stress $\sigma_{\max}$ in the bifurcation is restricted by some critical value $\sigma_{\max} \le \sigma^*$.

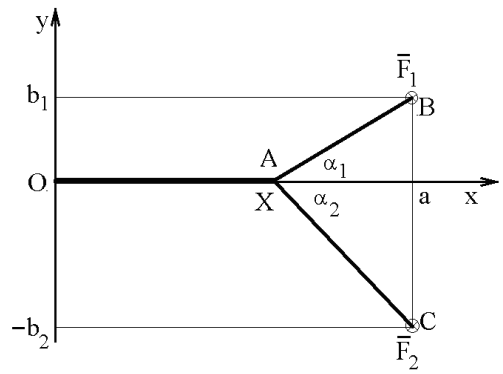

FIGURE 7 GEOMETRY OF THE BIFURCATION OA, AB, AC LOADED BY THE FORCES $\vec{F}_{1,2}$ APPLIED ON THE BIFURCATION IN B,C PERPENDICULARLY TO THE PLANE 0XY

The criterion (7) must be important for rigid branches of trees, bushes and shoots (Zamir and Medeiros, 1982), while for the leaf branches the total lateral surface provided the fluid delivery to the distributed customers (live cells) can be more important.

$$\Xi = \pi\left(d_0 L_0 + d_1 L_1 + d_2 L_2\right), \tag{8}$$

Stress distribution is determined by the bending moment $M = \sigma J / h$, where for the uniform circular bar h is the radius of the cross section. Since the maximal bending moments are produced in the cross sections at maximal distance to the applied forces, for the three bars composing the bifurcations the maximal stresses will be reached at the section O of the first bar, and the section a of the second and thirds bars. Then the restriction on the maximal stress will give the inequalities

$$\begin{aligned} M_{1\max} &= F_1 L_1 \le \frac{\pi}{32}\sigma^* d_1^3, \\ M_{2\max} &= F_2 L_2 \le \frac{\pi}{32}\sigma^* d_2^3, \\ M_{0\max} &= (F_1 + F_2)a \le \frac{\pi}{32}\sigma^* d_0^3. \end{aligned} \tag{9}$$

According to (9), the minimal values of $M_{1\max}$, $M_{2\max}$, and $M_{0\max}$ will be given by minimal diameters, so we can come from (9) to the equalities

$$d_1 = \sqrt[3]{\frac{32 F_{1,2} L_{1,2}}{\pi\sigma^*}}, \qquad d_0 = \sqrt[3]{\frac{32(F_1 + F_2)a}{\pi\sigma^*}}. \tag{10}$$

Since $L_{1,2} = \sqrt{(a - X)^2 + b_1^2}$, $L_0 = X$, substitution (9) in (7) and (8) gives the following criteria in the non-dimensional form

$$\Theta_{I,II} = k_{I,II}\Big(f^{n_{I,II}}((1-\chi)^2 + \beta_1^2)^{m_{I,II}} + \\ + ((1-\chi)^2 + \beta_2^2)^{m_{I,II}} + \chi(f+1)\Big), \quad (11)$$

where $\chi = X/a,\ \beta_{1,2} = b_{1,2}/a$, $f = F_1/F_2$, $n_I = 1/3, n_{II} = 2/3$, $m_I = 4/6, m_{II} = 5/6$, $k_I = \sqrt[3]{\frac{32\pi^2 a^4 F_2}{\sigma *}}$, $k_{II} = \sqrt[3]{\frac{16\pi a^5 F_2^2}{(\sigma*)^2}}$, (I) and (II) correspond to the criteria (8) and (7) accordingly.

Optimal location X of the bifurcation for the given geometry (a, b_1, b_2) and mechanical load (F_1, F_2) can be found from the conditions

$$\left(\Theta_{I,II}\right)'_{\chi} = 0, \quad \left(\Theta_{I,II}\right)''_{\chi\chi} > 0 \quad (12)$$

The branching ratio K, the optimal Murray parameter μ and the optimal bifurcation angles $\alpha_{1,2} = \frac{1-\chi}{\sqrt{(1-\chi)^2 + \beta_1^2}}$ can be computed then and compared to the measured values presented in the previous chapter. Since the real load on the branching plant structures includes own body mass, the payload (leaf mass), the wind, rain and snow load, the force distribution ($\vec{F}_1, \vec{F}_2$) must be insignificant and only the force asymmetry f might be important in connection of development the symmetric or quite asymmetric branches. Geometry of the bifurcation can also be described by relative parameters $(b_1 + b_2)/a \in]0,2[,\ b_1/b_2 \in]0,1[$.

RESULTS AND DISCUSSIONS

Direct computations by (10), (11) at known $a, b_{1,2}, F_{1,2}$ give algebraic equation for determination the optimal location of the branching point x=X. Numerical computations have been carried out for the symmetric area $b_1 + b_2 = a$ and two non-symmetric areas $b_1 + b_2 = a/2$ and $b_1 + b_2 = 2a$. Three values of the force asymmetry f have been chosen: f=0;2;0.5. Due to the symmetry the values $\beta_1 = 0.1;0.2;0.3;0.4;05$ have been used. Location of the optimal bifurcation point A in dimensionless coordinate $\chi = X/a$ at different area geometry and force distributions are presented in Fig.8.

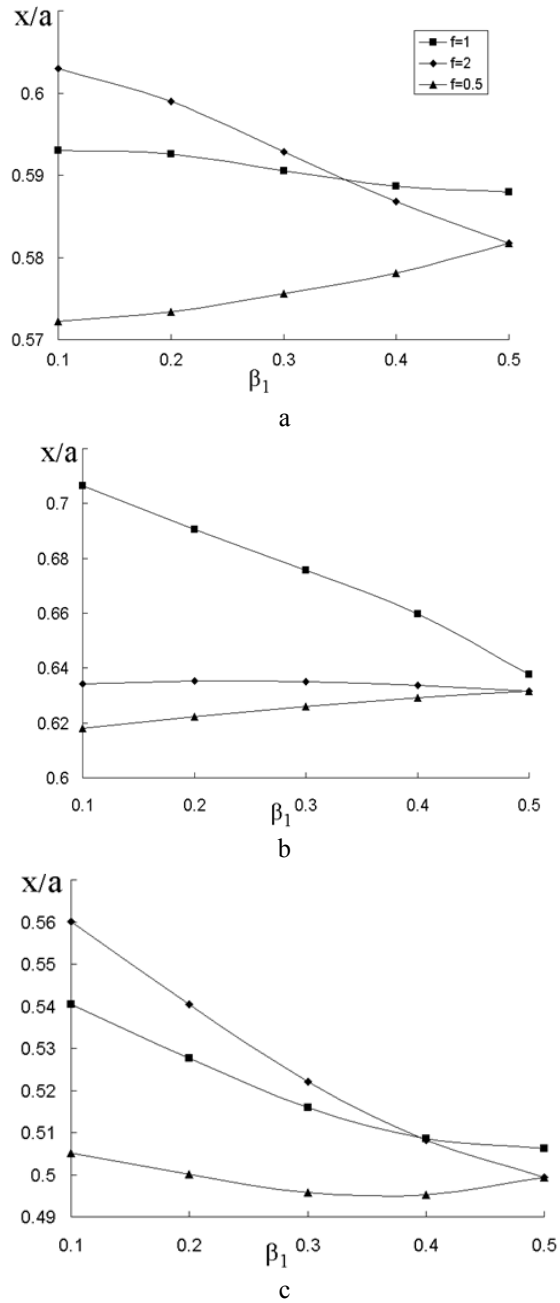

FIGURE 8 LOCATION OF THE OPTIMAL BIFURCATION POINT AT DIFFERENT $\beta_1 \in [0.1;0.5]$ AT $b_1 + b_2 = a$ (A), $b_1 + b_2 = a/2$ (B), $b_1 + b_2 = 2a$ (C). SQUARE, RHOMB AND TRIANGLE SIGNS CORRESPOND TO THE FORCE ASYMMETRIES F=1, F=2 AND F=0.5 ACCORDINGLY

Location of the point A exhibit quite small variations $0.57 < \chi < 0.61$ for the symmetric area $b_1 + b_2 = a$, $0.61 < \chi < 0.71$ for the elongated area $b_1 + b_2 = a/2$, and $0.5 < \chi < 0.57$ for the widened area $b_1 + b_2 = 2a$. When the area is elongated, the main branch OA must be longer, while for the widened area is shorter, which is physical. The difference between the corresponding averaged values is $\pm 4.5\%$ only. For the symmetrical location of the main branch OA ($\beta_1 = 0.5$) the two non-symmetric force distributions f=2;0.5 give the same solution which is natural. The values computed for the symmetrical loaded branch (f=1, $\beta_1 = 0.5$) correspond to the results obtained in [12]. The stability problem for the loaded branching structures composed of straight roads has been studied in (O'Reilly and Tresierras, 2011). The differences between the optimal location of the bifurcation point A at two non-symmetric loads (f=2;0.5) are bigger for the asymmetric location of the main branch OA ($\beta_1 = 0.1$) and smaller for its symmetric location ($\beta_1 = 0.5$) (Fig.9). It is obviously, the difference will increase for more asymmetric force distributions f=3;1/3;4;1/4;… . In some cases the values X/a are close to the golden ratio $X/a \approx 0.6$. Geometries of the optimal branches are depicted in fig.11 for the most asymmetric ($\beta_1 = 0.1$) and symmetric ($\beta_1 = 0.5$) cases. Location of the bifurcation point A at different sets of the force asymmetry f and $0.1 < \beta_1 < 0.5$ are filled by grey colour.

Since in the optimal branching the applied forces determine thicknesses of the beams or diameters of the cylindrical rods, the corresponding diameters can be computed from (7) at different model parameters. The asymmetry coefficient ξ, branching ratio K and Murray's coefficient μ can also be computed. The branching ratio and Murray's coefficient describe rather transport properties of the bifurcation of the rigid tubes for the fluid flow than to the stress minimization. According to (1), when $\mu \sim 1$ the bifurcation is closer to the optimal one. The branching angles $\alpha_{1,2}$ can be computed from the calculated values χ for any given geometry (fig.7). The computed dependency $\alpha(K)$ where $\alpha = \alpha_1 + \alpha_2$ is presented in fig.10a. Three sets of data corresponded to different geometry of the area are clearly visible.

Inside each set the three sets correspondent to different force asymmetry are clear separated only in the case $b_1 + b_2 = 2a$ with bigger branching angle α and branching coefficient K. There is quite good approximation of the general data $K = k_1 \exp(k_2 \alpha)$ (R^2=0.688) depicted in fig.10a by the solid line. The computed dependence is very close to those measured on the plant leaves (Kizilova, N., 2004a).

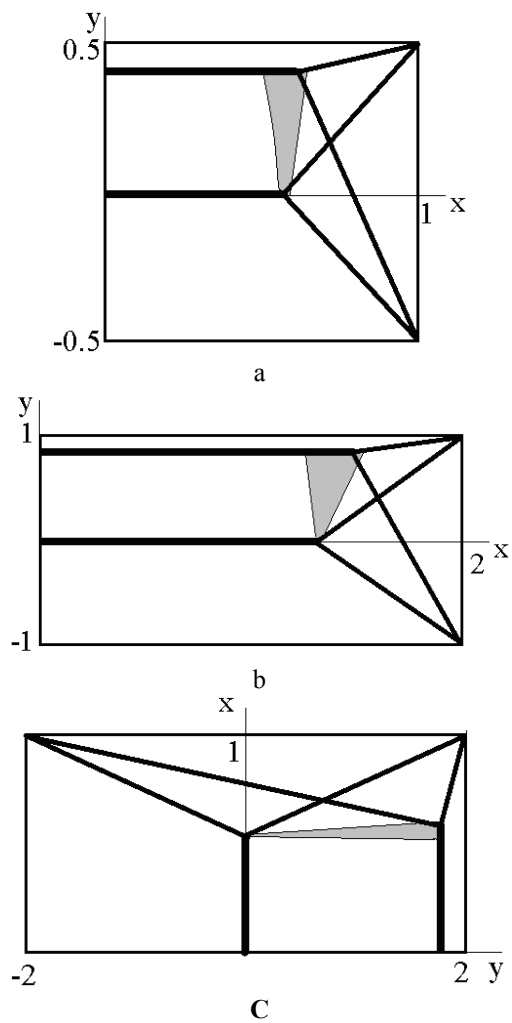

FIGURE 9 LOCATION OF THE BIFURCATION POINT ON THE AREA $x \in [0,a], b \in [-b_2, b_1]$ AT DIFFERENT BIFURCATION ASYMMETRY $\beta_1 \in [0.1, 0.5]$ AND AREA GEOMETRY

$b_1 + b_2 = a$ **(A),** $b_1 + b_2 = a/2$ **(B),** $b_1 + b_2 = 2a$ **(C)**

If we compare the branching angle α optimal for the stress minimization in the structure and the branching angle α^* computed for the same diameters from (2) and optimal for the fluid delivery along the branch, we shall obtain quite good correlation between them (fig.10b). It means both optimal solutions are quite close to each other. Taking into account the computed influence of small deviations of location of the branching point A in the area which corresponds to $\pm 5\%$ additional energy lost (Kizilova, 2004b), in nature the scatter of the data around the line $\alpha^* = \alpha$ (solid line in fig.10b) correspond to rather small energy lost compensated by optimality to some other external conditions or internal properties.

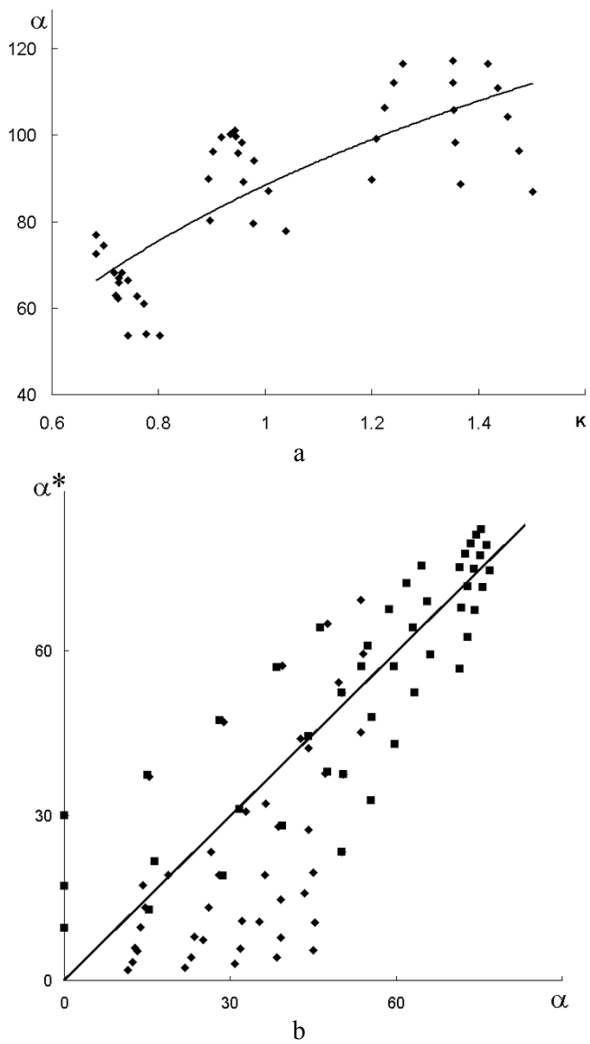

FIGURE 10 DEPENDENCIES $\alpha(\mathrm{K})$ (A) AND $\alpha^*(\alpha)$ (B). THE SQUARE AND RHOMB SIGNS IN (B) CORRESPOND TO THE LONGER (AC) AND SHORTER (AB) RODS ACCORDINGLY

The dependence $\mu(\mathrm{d}_1/\mathrm{d}_2)$ presented in fig.11a is similar to the measured dependencies $\mu(\mathrm{d}_0)$ and $\mu(\xi)$ (Kizilova, N., 2004a). The thicker the main branch, the closer the optimality coefficient to 1, while the small branches demonstrate bigger scatter around the optimal value. In the experimental data $0<\xi<1$, while in fig.11b $\mathrm{d}_1/\mathrm{d}_2$ could be bigger than 1, because in the cases when the shorter rod is loaded by the bigger force, in the optimal case it is thicker than the less loaded longer branch. In this cases diameter ratios of the shorter and longer branches may give values $\mathrm{d}_1/\mathrm{d}_2>1$.

Quite strong dependence $\alpha_2=\kappa_1\ln(\mathrm{M}_0)+\kappa_2$ (R^2=0.864) of the branching angle of the longer branch on the total bending moment M_0 appeared in the main rod has been found (fig.11b), while the shorter branch exhibits some noticeable scatter around the exponential averaged values (straight line in fig.11b) depending on the applied forces and initial branch asymmetry. The data measured on the vascular beds demonstrated the same dependence, as if the main daughter branch follows the diameter of the parent branch, while the smaller daughter branch has more freedom for branching and, therefore, the bigger scatter.

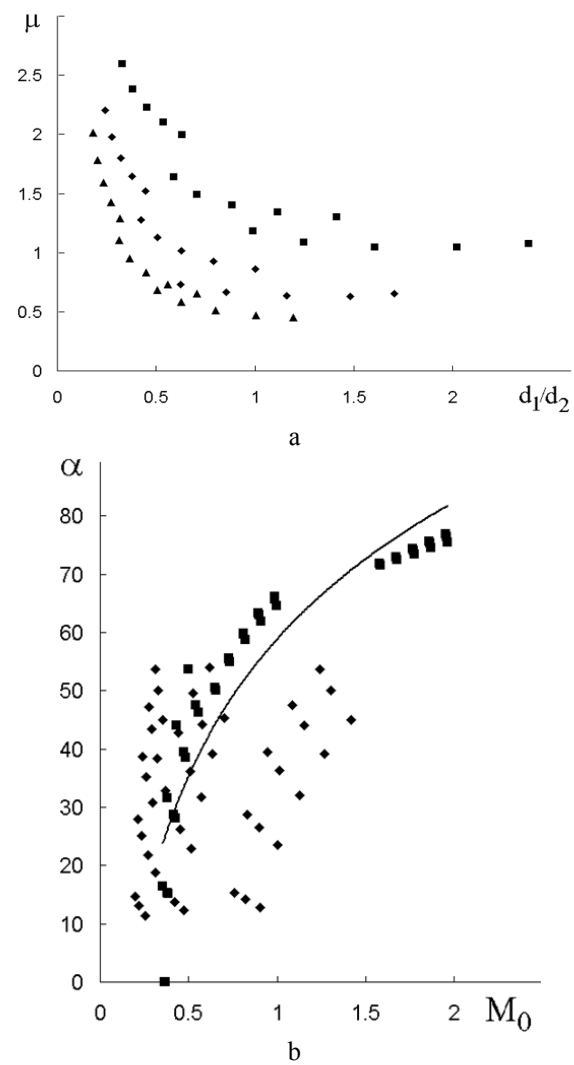

FIGURE 11 DEPENDENCIES $\mu(\mathrm{d}_1/\mathrm{d}_2)$ (A) AND $\alpha(\mathrm{M}_0)$ (B) COMPUTED FOR THE BIFURCATING BEAMS

In that way, the computed configurations of the optimal bifurcating fibres experienced minimal internal stress at given asymmetric load can be used for reinforcement of the tissue-like engineered composites in the woven or layered (fig.3) patterns, as well as 3D structures reinforcing convex shells (containers, capsules, roofs, pavilions, panels, etc).

The branched structures composed from nanotubes are perspective for optimal reinforcement of microscopic objects like artificial cells, tissue substitutes, MEMS units, fuel cells and others. Modern technologies allow synthesis of carbon, metal, polymer and other branched Y-shaped conjugations of nanotubes that can be used for simultaneous strengthening of the unit and delivery and distribution of macro- and nanofluids through them. The aerosol technique based on spray of a catalyst-precursor solution composed of metal salts in water directly into a furnace is a low-cost technology for obtaining Y-shape nanotubes and more complex branched structures of them (Heyning, Bernier and Glerup, 2005). The Y-shaped carbon nanotubes can be obtained by the arc discharge method (Osvatha, Koosa, Horvatha, 2003) and used for the reinforcement and heat conductivity purposes. The Y-shape TiO_2 nanotubes have been obtained by multi-step sonoelectrochemical anodization method (Mohapatra, 2008). Being embedded into a viscoelastic matrix with needed thermomecanical or electromechanical properties, the structures form new composites reinforced by a branching network of tubes. Many micro-units like liquid-based micro-coolers and heaters, fuel cells, artificial cells, molecular motors, lab-on-a-chip need permanent delivery of the working substances and taking away the products of reactions/decay, assimilates, and useful produced substances that can be fulfilled by the same elements which provide strengthening. It is a reasonable way for economy of the material and lightweight design of the micro- and nanosystems by double exploitation of the same system whose design provides optimality for both mechanical and transportation properties.

The diameters of the nanotubes in the manufactured Y-shape junctions are usually constant or uniform dependently on the material, and the branching angles are determined by the technological conditions and could be far from optimal ones in the above discussed meaning. Recently novel approaches for the controlled branching of the nanotubes by nucleation their lateral surface with a catalyst and, therefore, initiation of the branched growth have been proposed (Gothard, 2004). This will allow manufacturing of the branched structures of nanotubes as reinforcing structures that provide multicriteria optimization of the mechanical, heat and flow conductivity properties of the corresponding composite materials.

CONCLUSIONS

Natural materials in tissues and organs of plants and animals are mostly presented by fiber reinforced composites. The reinforcing fibers, from nano to macro scales, are branched systems of tubes or rods that exhibited certain geometrical regularities between the diameters and branching angles at the bifurcations, diameters and lengths in the general network. Statistical analysis of the measurement data obtained on the vascular beds of human and animals, as well as tree branches and leaf venation systems revealed the same regularities in their geometry. Solution of the optimization problem for the stationary fluid flow in rigid cylindrical tube when the total energy expenses for the viscous flow and metabolism are minimal gives the Murray's law. In that way, transportations networks in live nature are optimal pipelines provided minimal energy costs for transport and metabolism. Solution of similar optimization problem for the fluid percolation through the cylindrical tube with permeable wall at the assumption of the long thing tubes (d/L<<1) has the same form (Kizilova, 2005). As is was shown in the present paper, the optimal rigid Y-shape rods fastened at the beginning of its parent rod and loaded by non-symmetric forces reveal the distributions between diameters, branching angles and lengths that posses certain regularities similar to those obtained on the measured data.

Basing on the theoretical results, the obtained regularities are proposed for fabrication of the branching structures of nano/microtubes as reinforcing systems for the composite materials with optimal properties. Those materials will provide multicriteria optimization of their mechanical (strengthening), heat and flow conductivity (transportation) properties. Due to similarity of the solutions of both the mechanical and transportation problems, significant economy of the materials and lightweight design could be reached, which is especially important for the micro heaters/coolers, microfluidic separators/homogenizators, fuel cells, artificial cells and tissues, microengines and other MEMS units.

NOMENCLATURE

d_0 - diameter of the parent branch;

$d_{1,2}$ - diameters of the daughter branches;

F – force;

h - distance to the axis;

J - moment of inertia;

L – length;

$K = \dfrac{d_1^2 + d_2^2}{d_0^2}$ - branching ratio;

M – moment of force;

R – radius;

Q - volumetric flow rate;

$\vec{q}$ - heat flux;

T – temperature;

Z - Poiseuille resistivity for the steady flow;

α_1, α_2 - branching angles of the daughter branches;

$\alpha = \alpha_1 + \alpha_2$;

η - fluid viscosity;

λ - thermal conductivity;

$\mu = \dfrac{d_1^3 + d_2^3}{d_0^3}$ - optimal Murray parameter;

$\xi = \frac{\min\{d_1, d_2\}}{\max\{d_1, d_2\}}$ - asymmetry coefficient;

σ - stress;

τ - relaxation time;

τ_w - wall shear stress (WSS);

χ - parameter in the heat equation.

REFERENCES

1. Fung, Y.C., 1981. *Biomechanics: Mechanical Properties of Living Tissues*. NY: Springer-Verlag.
2. Kizilova, N.N. and Posdniak, L.O., 2005. Biophysical mechanisms of long-distance transport of liquids and signaling in high plants. Biophysical Bulletin, 15(1), p.99-103.
3. Murray, C.D., 1926. The physiological principle of minimum work. I. The vascular system and the cost of blood volume. *Proc. Nat. Acad. Sci. USA*, 12, pp.207-214.
4. Murray, C.D., 1926. The physiological principle of minimum work applied to the angle of branching of arteries. *J. Gen. Physiol*., 9, pp. 835–841.
5. Rosen, R., 1967. *Optimality Principles in Biology*. NY: Plenum Press.
6. Weibel, E.R., 1963. *Morphometry of the human lung*. NY:Academic.
7. La Barbera, M., 1990. Principles of design of fluid transport systems in zoology. *Science*, 1000, pp. 249-252.
8. Kizilova, N. and Popova, N., 1999. Study on transportation systems of plant leaves. *Probl. Bionics*, 51, pp. 71-79.
9. McCulloh, K.A., Sperry, J.S. and Adler, F.R., 2003. Water transport in plants obeys Murray's law, Nature, Vol. 421, pp.939-942.
10. Kizilova, N., 2008. Common Constructal Principles in Design of Transportation Networks in Plants and Animals. In: A.Bejan, G.Grazzini, eds. *Shape and Thermodynamics*. Florence: Florence Univ. Press. pp. 1-12.
11. Zaragoza, C., Márquez, S. and Saura, M., 2012. Endothelial mechanosensors of shear stress as regulators of atherogenesis. *Curr Opin Lipidol*., 23, pp. 446-52.
12. Chernousko, F.L., 1977. Optimal structure of branching pipelines. *Appl. Mathem. Mech*, 41, pp.376-83.
13. Kizilova, N., 2005. Hydraulic Properties of Branching Pipelines with Permeable Walls. *Intern. J. Fluid Mech.Res*., 32, pp.98-109.
14. Kizilova, N., 2004. Computational approach to optimal transport network construction in biomechanics. *Lecture Notes in Computer Sci*., 3044, pp.476-85.
15. Leelavanichkul, S. and Cherkaev, A., 2004. Why grain in tree's trunks spiral: mechanical perspective. *Struct. Multidisc. Optimiz*., 28, pp.127–135.
16. S.C. Cowin, ed., 1989. *Bone Mechanics*, Boca Raton; CRC Press.
17. Kizilova, N., 2012. Mathematical modelling of biological growth and tissue engineering. In: R. Bedzinski, and M. Petrtyl, eds. *Current trends in development of implantable tissue structures*, Warsaw: IBB Press, pp.18-27.
18. Fukada, E. and Yasuda, I., 1957. On the piezoelectric effect in bone. *J. Phys. Soc. Japan*. 12, pp.1158-1162.
19. Avdeev, Yu.A. and Regirer, S.A., 1985. Electromechanical properties of bone tissue. In: *Modern problems of biomechanics*. Riga; Zinatne, 2, pp.101-131.
20. Langer, K.. 1861. Zur Anatomie und Physiologie der Haut. Über die Spaltbarkeit der Cutis. *Sitzungsbericht der Mathematisch-naturwissenschaftlichen Classe der Wiener Kaiserlichen Academie der Wissenschaften Abt*., pp.44-54.
21. Kramer, E.M., 2002. A mathematical model of pattern formation in the vascular cambium of trees. *J. Theor. Biol*. 216, pp. 147-159.
22. Holzapfel, G.A., Gasser, Th.C. and Ogden, R.W., 2006. A New Constitutive Framework for Arterial Wall Mechanics and a Comparative Study of Material Models. *J. Elasticity*, 61, pp. 1-48.
23. Birk, D.E., Southern, J.F., Zycband, E.I., et al., 1989. Collagen fibril bundles: a branching assembly unit in tendon morphogenesis. *Development*, 107, pp.437-443.
24. Brownfield, D.G., Venugopalan, G., Lo, A., et al., 2013. Patterned collagen fibers orient branching mammary epithelium through distinct signaling modules. *Curr. Biol*., 23, pp.703-709.
25. Kizilova, N., 2011. Geometrical regularities and mechanical properties of branching actin structures. In: Nanobiophysics, Kharkov:IM Press, pp.141-146.
26. Schwendener, S., 1874. *Das mechanische Prinzip in anatomische Bau der Monokotylen mit verleichenden Ausblicken auf die übringen Pfanzenklassen*, Leipzig.
27. Schwendener, S., 1878. *Die mechanische theorie der blattstellungen*, Leipzig.
28. Honda, H., 1978. Tree branch angle: maximizing effective leaf area, *Science*, 199, pp. 888-889.
29. Niklas, K.J. and Spatz, H.-Ch., 2004. Growth and hydraulic (not mechanical) constraints govern the scaling of tree height and mass. *Proc. Nat. Acad. USA*., 101, pp. 15661–3.
30. Yarin, A.L., Kataphinan, W. and Renekera, D.H., 2005. Branching in electrospinning of nanofibers. *J. Appl. Phys*. 98, p.064501.
31. Gevorkyan, A., Shter, G.E., Shmueli, Y., et al., 2014. Branching effect and morphology control in electrospun $PbZr_{0.52}Ti_{0.48}O_3$ nanofibers. *J. Mater. Res*., 29(16), pp. 1721-9.
32. Aggarwal, D., Matthew, H.W.T., 2009. Branched chitosans II: Effects of branching on degradation, protein adsorption and cell growth properties. *Acta Biomaterialia*, 5, pp. 1575–81
33. Boskovic, B.O., Stolojan, V., Zeze, D.A., et al., 2004. Branched carbon nanofiber network synthesis at room

temperature using radio frequency supported microwave plasmas. *J. Appl. Phys*., 96(6), pp. 3443-6.
34. Heyning, O.T., Bernier, P., Glerup, M., 2005. A low cost method for the direct synthesis of highly Y-branched nanotubes. *Chemical Phys. Lett*., 409, pp. 43–47.
35. Alvarez, F.X., Jou, D. and Sellitto, A., 2009. Phonon hydrodynamics and phonon-boundary scattering in nanosystems. *J.Appl.Phys*., 105(1), p.014317.
36. Zamir, M. and Medeiros, J.A., 1982. Arterial branching in man and monkey. *J. Gen. Physiol*., 79, pp.353–360.
37. O'Reilly, O.M. and Tresierras, T.N., 2011. On the static equilibria of branched elastic rods. Intern. J. Engin. Sci., 49, pp. 212–27.
38. Kizilova, N., 2004. Optimization of branching pipelines on basis of design principles in Nature. In: *Proc. of the ECCM Congress on Computational Methods in Applied Sciences*, Finland, 1, pp.237-48.
39. Heyning, O.T., Bernier, P. and Glerup, M., 2005. A low cost method for the direct synthesis of highly Y-branched nanotubes. Chemical Phys. Lett., 409, pp. 43–47.
40. Osvatha, Z., Koosa, A.A., Horvatha, Z.E., et al., 2003. STM observation of asymmetrical Y-branched carbon nanotubes and nano-knees produced by the arc discharge method. *Materials Sci. Engin*., 23, pp. 561–4.
41. Mohapatra, S.K., Misra, M., Mahajan, V.K. and Raja, K.S., 2008. Synthesis of Y-branched TiO2 nanotubes. *Materials Letters*, 62, pp. 1772–4.
42. Gothard, N., Daraio, C., Gaillard, J., et al., 2004. Controlled Growth of Y-Junction Nanotubes Using Ti-Doped Vapor Catalyst. *Nano Letters*, 4, pp. 213-7.